Development and Implementation of an IoT Weather Station for Localized Meteorological Parameter Monitoring and Data Localization

Adeniran, A.O.[1], Ukabrinachi, E.I.[2]

[1&2]Department of Physics, University of Uyo

DOI: https://doi.org/10.51584/IJRIAS.2026.11030084

Received: 06 March 2026; Accepted: 12 March 2026; Published: 14 April 2026

ABSTRACT

Continuous, high-precision air measurement in off-grid and resource constrained environments is a major challenge in the fields of environmental science, precision agriculture, and climate studies. The development of Internet-of-Things (IoT) and renewable energy technologies has introduced significant advances to the creation of autonomous and affordable monitoring of meteorological parameters, in particular to detect weather phenomena in Nigeria. As a counter measure, this paper designed, built, and deployed a solar-powered weather station, which uses ESP32 microcontroller to read and record local weather conditions in the atmosphere. The sensor package included a DHT11 thermistor-humidity sensor, an MQ135 particulate-matter sensor, an IR fog detector, a rainfall-intensity gauge, and an LDR to measure the solar irradiance and darkness. The transmission of real-time data is done through the Blynk dashboard and Google Sheets simultaneously with the presentation of numeric values on a specific LCD display. All sensor modules yielded the same results according to the requirements of the manufacturers in the laboratory and in the field. The I2C LCD was able to cycle through all the parameters screens. The ESP32 had also been very stable in terms of Wi-Fi connectivity and was also very efficient when it came to transmitting structured data to the Blynk server as well as the Google sheets endpoint where timed records of the environmental variables were recorded in real time. The LM7805 voltage regulator provided a constant 5.01V -0.03V at the entire input voltage of the solar charging subsystem. The noise of analog sensors was reduced to reasonable values of measurements by applying a 20-sample moving-average hardware filter. Performance measures were measured in the field under natural conditions and found that the performance metrics showed high correlation in temperature and relative-humidity measurements, effective fog detection, consistent rainfall status measurements and accurate irradiance measurements. The system was fully initialized and was successful in data transfer (98 percent) in both Google Sheets and the Blynk dashboard. This platform has thus been easily implemented in agricultural, meteorological and environmental management applications without requiring infrastructure other than a local access point of Wi-Fi.

Keywords: IoT, ESP32, Atmospheric monitoring; Renewable energy, Google Sheets, Blynk, environmental sensing, DHT11, MQ135 , Photoconductive, real time, Sensors, Nigeria

INTRODUCTION

Reliable atmospheric information is essential to evidence-based decision making in the fields of agriculture, population health, development of urban infrastructure, and climate monitoring. The relatively high cost of conventional meteorological stations, typically exceeding USD50,000 per site without civil and maintenance contracts and telecommunication infrastructure, makes comprehensive spatial coverage unaffordable to most of the low- and middle-income countries and the institutions conducting the research on their behalf (Mainetti et al., 2019). It is expected that extreme environment and climate will have more and more extensive effects on the effectiveness and cost-effectiveness of all renewable energy systems (Sadorsky, 2021). This is because the renewable energy in Nigeria is not developed due to the lack of the availability and reliable meteorological information. As a result, it is important that the current power-grid analysis is supported with sufficient, accurate, and real-time meteorological information (Ogunjuyigbe et al., 2016). Smart weather stations are data collection devices, which automatically detect data about weather and environmental conditions and store it in the cloud

ISSN No. 2454-6194 | DOI: 10.51584/IJRIAS |Volume XI Issue III March 2026

or on a web server without the participation of a person (Kodali & Mandal, 2016). These systems are referred to as smart using Internet of Things (IoT) technology as opposed to the traditional weather stations, which are referred to as non-smart and tend to save the measurement data as a regular SD memory card, flash memory, or EEPROM memory (Agarwal and Agarwal, 2019). High-technology weather stations employ numerous meteorological sensors that measure and transmit the atmospheric parameters such as temperature, humidity, dew point, air pressure, direction and speed of the wind. Use a number of weather instruments to measure and compare weather parameters, such as temperature, relative humidity, dew point, atmospheric pressure, wind direction, and wind speed. The conventional weather monitoring system requires the use of skilled labor to operate and perform regular maintenance and may significantly increase the lifecycle cost of the weather station (WMO, 2018). The cost of obtaining specific and localized scientific weather data can be significantly reduced by the development of semiconductor technology because a wide range of various weather sensors are combined with microcontrollers (Ngu et al., 2020). The availability of the short-term weather forecasts is limited in many local communities across Africa (Dinku et al., 2018). The market of smart weather stations has been experiencing a tremendous demand which is due to the increased focus on climate change and the emergence of the need to gather more accurate meteorological information in various industries. Smarter weather stations have also been supported by technological advancements that provide real-time tracking, forecasting analytics, and a smooth relationship with other intelligent devices, finding more applications in agriculture, aviation, and transportation (MarketsandMarkets, 2023). According to market research, it is estimated that the global market of smart weather stations will continue its growth, and the businesses and stakeholders will have positive prospects (Lee et al., 2022). The recent development in the Internet of Things has revolutionized weather monitoring where traditional grid-dependent stations have been replaced with low-energy, self-solar monitoring systems. Innovations have modified weather surveillance systems, which were previously grid reliant and classical, and moved to low-power, solar-powered ones (Mekki et al., 2019). Brown et al. (2022) note the real-time cloud connection of smart stations based on ESP32 that reduces latency to approximately 1 second and power usage to 10 -A. Instant cloud connectivity of stations using ESP32, with minimal latency of about 1 second and power consumption of 10 -MW in the sleep state, outperforming wired systems. Nigeria NiMet 2025 IoT -LoRaWAN installations would reconciliate lack of urban data in Nigeria with WMO-compliant low-maintenance devices that are climate resilient. Sensor fusion Sensor fusion is common: the DHT11/DHT22 (± 0.5 to 2 0 C accuracy), MQ135 (2 to 3^0C error after burn-in NH_3/CO_2), BMP180 to measure pressure and LDR to measure irradiance. 12 -40 hours with Maximum Power Point Tracking (MPPT), suitable to low-power designs with 160mA in the active state and 10mA in the sleep state. Nigerian studies show that the estimates of renewable have problems caused by lack of sufficient data, and the prototype costs are below 100 dollars compared to 100 dollars. However, there are still weaknesses in limited fog/rain intensity in economic African systems, non-presence of integrated nocturnal hours, and high preheating requirements of the MQ135 (24-48hours).

METHODOLOGY

Inventory of Components and Their Functional Descriptions for the System

The hardware components utilized in the system are listed in Table 1.1 below:

Table 1.1: Components Inventory and Functions

	Component	Primary Function	GPIO / Interface	Protocol / Specification
	ESP32 Dev Board	Central MCU, Wi-Fi, ADC, I2C	Master controller	Wi-Fi 802.11 b/g/n; 240 MHz dual core
	DHT11 Sensor	Temperature & relative humidity	GPIO IO15	Single-wire digital; ±2°C / ±5% RH
	MQ135 Gas Sensor	Air quality / gas concentration	ADC pin (analog)	Analog SnO_2; detects NH_3, NO, CO_2, benzene
	IR Sensor	Fog and mist presence detection	GPIO IO32 (digital)	Active IR emission / photodetection; digital OUT
	LDR + 10 kΩ divider	Solar irradiance; darkness hours	ADC IO33 (analog)	CdS photoresistor; 12-bit SAR ADC

ISSN No. 2454-6194 | DOI: 10.51584/IJRIAS |Volume XI Issue III March 2026

	Rain Sensor	Rainfall intensity detection	ADC pin + digital OUT	PCB electrode + comparator; analog & digital
	16×2 LCD (I2C backpack)	Local real-time parameter display	SDA: IO21; SCL: IO22	PCF8574 I2C expander; 0x27 / 0x3F
	Red LED (×1)	System power-on status	GPIO IO16	Digital output; series current-limiting resistor
	Blue LED (×1)	Wi-Fi / Blynk connected indicator	GPIO IO17	Digital output; series current-limiting resistor
	Yellow LED (×1)	Active data upload indicator	GPIO IO2	Digital output; blinks on successful transmission
	12V PV Solar Panel	Primary solar energy source	Power input	Photovoltaic; feeds LM7805 and battery charger
	LM7805 Regulator	Regulated +5V DC supply to all electronics	Power regulation	Linear regulator; 1A max; thermal overload protection
	Rechargeable Battery	Energy storage and backup supply	In-circuit buffer	Lead-acid or Li-ion; 6–12 Ah; 12–40 h autonomy

ESP32 Development Board

The paper is a summary of various low-cost, low-power, systems on a chip (SoC) microcontrollers designed by Expressif Systems, the primary aim of which is to support Internet of Things (IoT) applications. The devices (Figure 1.0) also have integrated Wi-Fi as well as Bluetooth, thus making them especially appropriate in wireless communication within embedded systems. Every unit can be equipped with a dual-core 32-bit CPU (Alexander et al., 2019), which is one of the features that precondition the high performance that may be expected in modern IoT deployments.

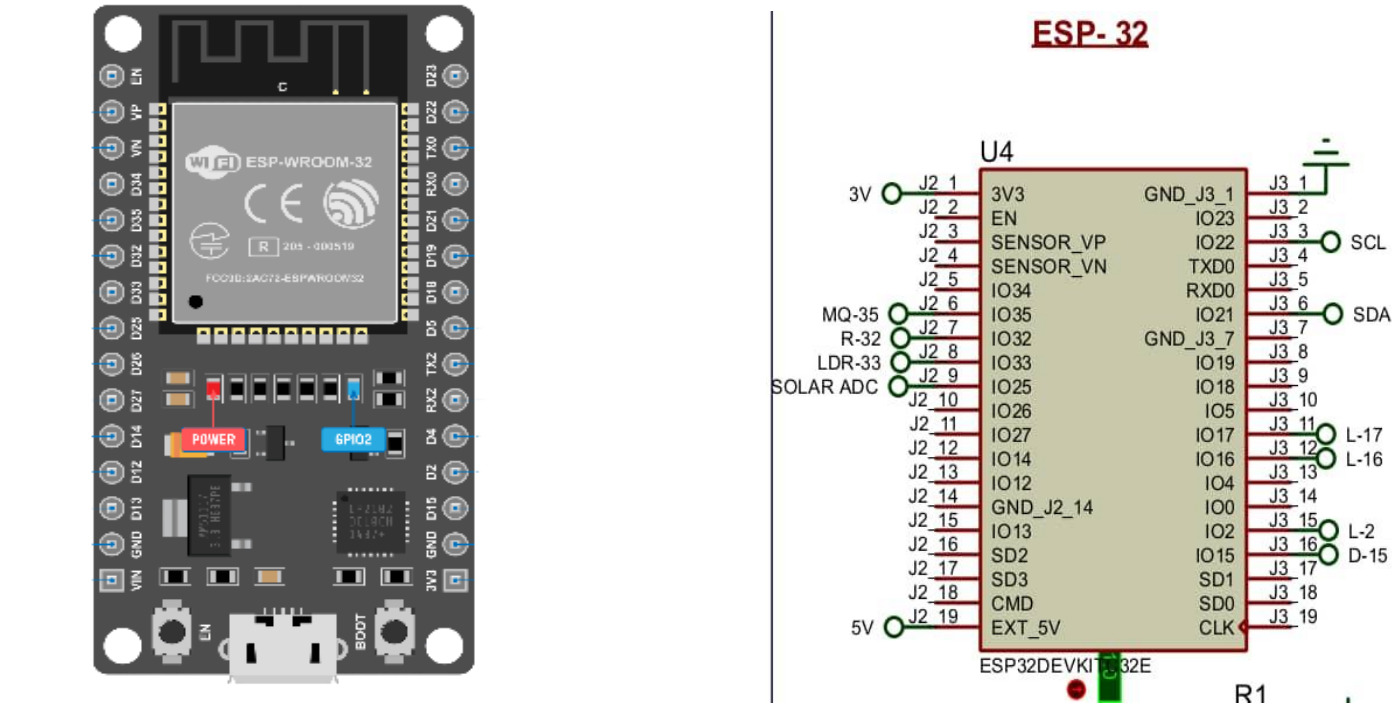

Figure 1.1: ESP32 Board and Internal Circuit

DHT11

The DHT11 (Figure 1.2) is a simple, but cheap, digital temperature-humidity sensor, commonly used in hobbyist applications and in industrial internet of things. It combines capacitive elements in humidity sensing, an NTC thermistor which measures temperature, and an internal 8-bit microprocessor which transmits calibration digital data through a single-wire serial interface. It is an architecture that makes it easier to integrate with conventional microcontrollers, including Arduino, ESP32, or Raspberry Pi. The sensor then delivers readings of ambient

ISSN No. 2454-6194 | DOI: 10.51584/IJRIAS |Volume XI Issue III March 2026

temperature and relative humidity as digital values straight to the ESP32 which will then be logged in the environmental data.

Figure 1.2: DHT11 Board and Internal Circuit

MQ135 Gas Sensor (Air Moisture / Air Quality)

Figure 1.3 is an example of a semiconductor gas sensor with the name MQ135, which uses a layer of tin dioxide (SnO_2). Electrical resistance of the sensor changes depending on the target gases such as ammonia (NH_3), nitrogen oxides (NO, NO_2, and NO_3) and benzene, smoke and carbon dioxide (CO_2) and has been listed as one of the main tools in measuring air quality and the composition of atmospheric gases. Secondary sensitivity is also found in the device to moisture-laden air conditions that are linked to events of high humidity. A voltage corresponding to the concentration of the gas in the air is generated; the voltage signal is measured at one of the ADC pins of the ESP32. The MQ135 needs a burn-in or pre-heat period, which ranges between 24 and 48 hours after the initial use to stabilize measurements and obtain them with reasonable accuracy (Lakshmikantha et al., 2019). This requirement of the conditioning step was a significant challenge when initial testing of the system was being done and was overcome by adding some time to the pre-conditioning period before calibration. The MQ135 also requires careful power control, especially under solar-powered operation, using high-voltage (5 V) and heater current (in the range of 150 mA). It has a wide detection capability, which allows it to be particularly used in extensive multi-gas environmental characterisation, thus increasing the ability of the system to monitor the quality of air in rural and peri-urban environments comprehensively (Rajab et al., 2021).

Figure 1.3: MQ135 System

IR Sensor (Fog Detection)

It (Figure 1.3) determines objects or obstacles by illuminating and accepting infrared light. In scholarly words, we consider this to be a proximity sensor and a reflectance sensor that is used to outline objects and obstacles. Its principle is based on active infrared emission and photo detection, namely, it emits infrared rays at a specific wavelength, and a photodiode detector is measured by the intensity of the reflected and scattered light (Venkatraman, 2017). Fog and mist can be defined as the presence of suspended water droplets which diffract the infrared radiation. As the density of the fog therefore increases the scattering coefficient of the medium also

ISSN No. 2454-6194 | DOI: 10.51584/IJRIAS |Volume XI Issue III March 2026

increases, hence resulting in a measurable increase in the diffuse reflection reflected by the infrared sensor. This effect forms the physical foundation of the fog sensors in the current meteorological system which makes use of infrared sensors. The IR sensors provide a digital signal which switches between a HIGH logic level (Fog Detected) and a LOW logic level (Clear Atmosphere) based on the sensitivity level set in the device. The sensor output is connected to IO32 on the ESP32 module that converts the digital signal into a binary number (Yes or No) that is shown by the system and sent to the Blynk cloud platform to be stored.

Figure 1.4: IR Sensor

An LDR (Light Dependent Resistor)

With modern solid-state device nomenclature, a component informally identified as a photoresistor is a completely passive element of semiconductor whose electrical resistance is probably decreasing with the incident photonic flux (Figure 1.4). Namely, the light-dependent resistor (LDR), made from semiconductor compounds, including cadmium sulfide (CdS), exhibits resistances of megohm scales, when untouched by the external light, and decreases to the kilo-ohm scales when being struck by the light, which recent literature has reported (Wahab et al., 2020). In the current system, the LDR will complete a twofold function: it will assess the solar irradiance levels to determine the adequacy of photovoltaic charging conditions and assess the solar availability in general, thus enabling the determination of nocturnal period by tracking intervals. The LDR is wired into a voltage-divider circuit using a 10k resistor to pull-down the voltage, the voltage-divider output voltage is then fed to the delta-cathode (DC) pin of an ESP32 microcontroller, which converts the analog level into a 12-bit resolution signal. Lastly, this digitalized voltage output is converted into a solar intensity index using an extreme firmware calibration and programmed specifics.

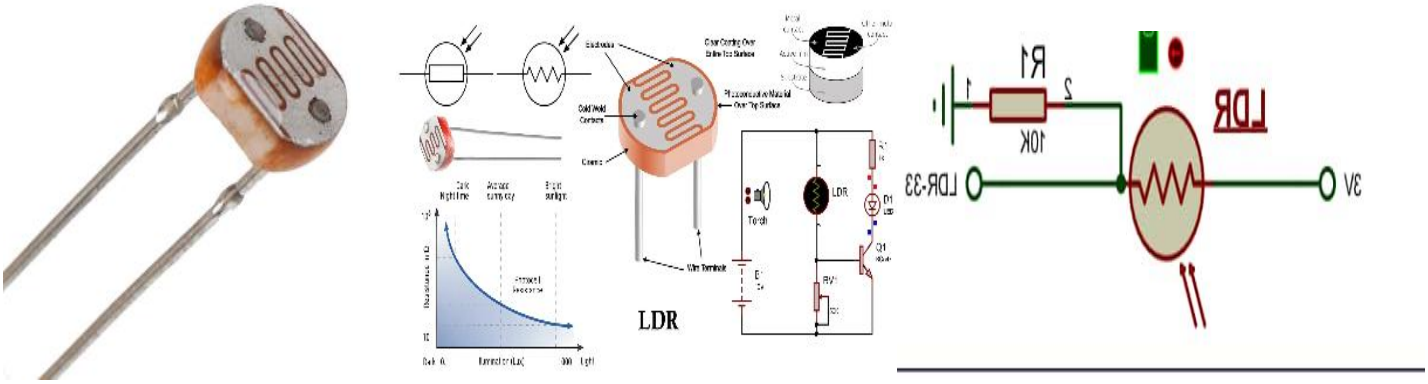

Figure 1.5: Light Dependent Resistor

Rain Sensor

The rain sensor module is a printed circuit board (PCB) module which includes a sensing pad in which the copper trace electrodes are exposed and includes a comparator circuit (Figure 1.6). Once the rain hits the electrodes, it completes the conductive circuit; resistance of such circuit is dependent on the intensity of the rainfall. When the amount of precipitation is increased, these augments bridging between electrodes thus decreasing the resistance and increasing the analog output voltage. The intensity of rainfall is proportional to this voltage which is measured through the ESP32 ADC pin. The ESP32 also produces a digital signal which activates when the

ISSN No. 2454-6194 | DOI: 10.51584/IJRIAS |Volume XI Issue III March 2026

amount of rain falls beyond a specified jumper point comparator threshold, giving crude presence/absence sensing. The system, therefore, uses analog and digital output to measure the intensity of the rainfall and to detect rainfall occurrences to analyze the precipitation pattern.

Figure 1.6: Rain sensor module and Internal Circuit

16×2 LCD Display with I2C Interface:

The LCD 16 x 2 (Figure 1.7) panel provides real time visual display of sensor data in character form with 16 alpha numeric characters per line. The display includes the I2C communication channel as it connects with the ESP32 with the serial data line (SDA), which is linked to ESP32 pin 21, and the serial clock line (SCL), which is linked to ESP32 pin 20 (Mathivanan et al., 2020). The LCD has a standard I2 C address - standard 0x27 or 0x3F - and at the same time it provides real-time temperature, humidity, sunlight, fog sensors and rains detectors readings, which are programmed through the Liquid Crystal I2 C library. The fact that it can perform local display makes sure that operational information can be accessed even when the network is offline or Blynk is disconnected.

Figure 1.7: LCD 16 by 2

LEDs

The system involves three LED (Figure 1.8) indicators which provide a visual status interface in light emitting diodes and therefore it does not need an LCD or smartphone applications. The red LED has a connection to a GPIO pin and indicates that there is power in the system; the LED being on is confirmation that the solar power

ISSN No. 2454-6194 | DOI: 10.51584/IJRIAS |Volume XI Issue III March 2026

system and the voltage regulation circuit are functioning correctly and that the correct voltage is being delivered to the ESP32 and all the sensors connected to it. The blue LED shows that the Wi-Fi connection is successful and the device is communicating with the Blynk IoT server; the blue LED turned off notifies the user that he has a network connection issue. The yellow LED indicates that the system is in action mode to receive sensor data and publish values on the Blynk cloud.

Figure 1.8: LED Indicator

Circuit Analysis

The circuit is precisely designed to fit together the basic components, including sensors, ESP32 microcontroller, a display module, and a full-fledged power subsystem.

Power Supply Path:

This subsystem forms the backbone of the weather station, which ensures provision of continuous power supply and thus this allows autonomous functioning in off-grid data-monitoring cases. A 12V photovoltaic array, a specific charge controller and a voltage-regulation stage which uses LM7805 regulator to reduce the supply to a fixed 5V which is required by the equipment are included in the power delivery chain. To reduce high-frequency ripples, eliminate transient spikes and eliminate oscillatory behaviour. A rechargeable lithium-ion battery is used to achieve energy storage. The ESP32 is supplied through its 5V input pin, and peripheral sensors, such as the DHT11, LCD, IR, MQ135 and LED, are supplied on the 5V rail provided by the LM7805. The LDR is connected to one end of a voltage divider with a 10ohms resistor and connected to ESP32 pin analog-to-digital converter 1033. LM7805 is a three-terminal positive voltage regulator that includes up to 1A of output current and includes short circuit and thermal overload protection (Texas Instruments, 2023).

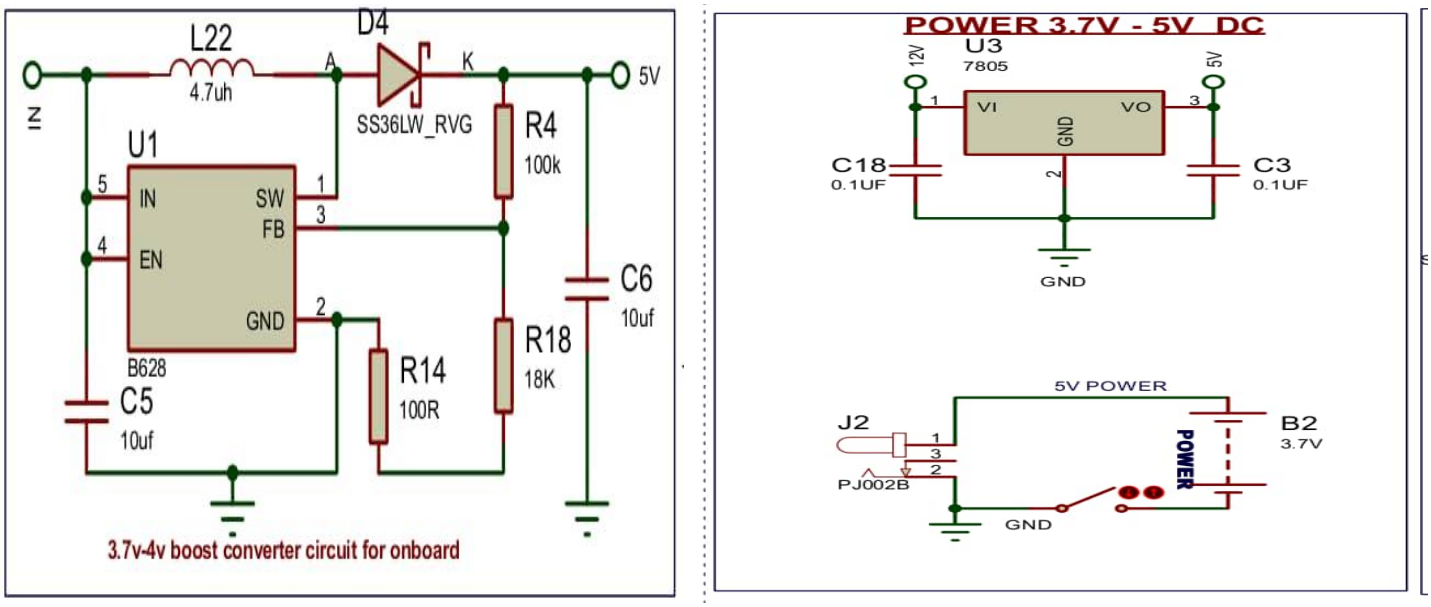

Figure 1.9: Power Supply Unit with charge controller

ISSN No. 2454-6194 | DOI: 10.51584/IJRIAS |Volume XI Issue III March 2026

Sensor Connections to ESP32:

Figure 2.0 illustrates all the connections between all sensors and the ESP32 microcontroller that is the main controller that processes the signals sent by each sensor. DHT11 is a temperature/humidity sensor that is linked to the IO15 digital data pin. The single-bus communication protocol is proprietary and needs a time-accurate control, which is met by the ESP32 DHT library, which uses timer functions at a microsecond accuracy (Kolban, 2018). The rain sensor has an analog output of the analog sensor and is connected to one of the analog sensors input pins of the ESP32. The 12-bit SAR ADC in the device provides 4096 discrete values of a 0-3.3V input, which is sufficient to differentiate between changes in the intensity of rainfall on the sensor analog output voltage (Espressif Systems, 2023). The gas sensor MQ135 has an analog output connected to a pin of the ESP32 ADC. Since MQ135 requires a lot of current in the form of an internal heater element (150mA on average), it is connected to the 5 V supply rail directly and not to a GPIO pin, though analog signal output is linked to ADC pin (Lakshmikantha et al., 2019).

The digital signal that the IR sensor produces is hooked to a digital input, GPIO pin IO32, which is a digital input, and the internal pull-up resistor is activated. Solar Intensity Solar Intensity is measured by connecting the output of the LDR voltage divider to ADC pin IO33. The signals of indicator LED drives are generated at the film of IO16 (red LED), IO17 (blue LED), and IO2 (yellow LED) with the corresponding current-limiting resistors to preserve the LEDs and the GPIOs. The I2C interface of the LCD connects the hardware I 2C peripheral pins, IO21 (SDA) and IO22 (SCL) of the ESP32, to the LCD.

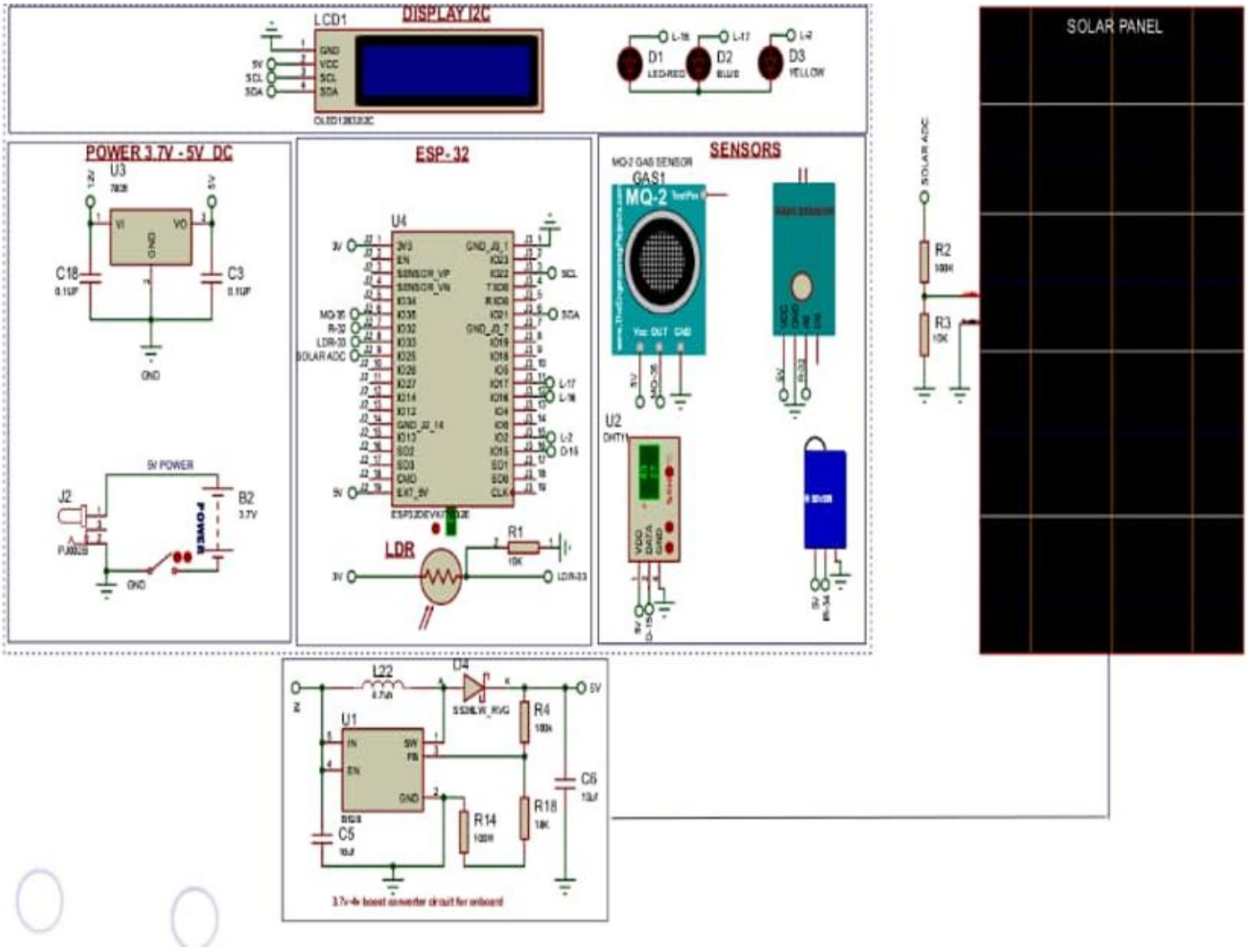

Figure 2.0: Constructed System Complete Circuit and Internal Circuit

Note: Each sensor has been assigned to an accessible GPIO or ADC channel on the ESP32 for optimal data acquisition.

ISSN No. 2454-6194 | DOI: 10.51584/IJRIAS |Volume XI Issue III March 2026

Exhibition and Internet of Things Integration

The liquid crystal displays integration is made using the ESP32 micro-controller with the I2C interface that is traditionally designed to work at 100 kHz and in fast mode at 400 kHz. It conforms to the I2C communication protocol and provides high level character printing functions. The bus address of the LCD is programmed in the software, and this makes the LCD persistent on power-cycle changes. The IoT integration of Blynk is enabled by the Wi-Fi module on the ESP32 to find a connection with a local 2.4 GHz wireless access point with the SSID and passwords encoded into the firmware. The gadget establishes a TCP connection with Blynk cloud server with a system authentication token. The frequency of data transmission is controlled by the Blynk.run() timer and an adjustable firmware-defined delay of 10-30 seconds, and in effect, balances the demand to have the freshest data transmitted with the API rate limitations of Blynk and the power consumption of Wi-Fi.

The yellow LED also lights up when successful transmission is achieved to show there is activity in data upload. The data of real-time sensors is available to users via the Blynk mobile apps and a Google Sheet.

	A	B	C	D	E	F	G	H	I	
1	TIMESTAND	TEMPERATURE	HUMIDITY	RAINFALL	RAIN STATUS	FOG	FOG VISIBILITY	AIR	AIR MOISTURE	DARK
788	2/21/2026 0:37:46	35.2 °C	57.0 %	0.0 mm	NO_RAIN	CLEAR	10.0 km	SAFE_AIR	0.2 g/m³	
789	2/21/2026 0:38:08	35.2 °C	57.0 %	0.0 mm	NO_RAIN	CLEAR	10.0 km	SAFE_AIR	0.2 g/m³	
790	2/21/2026 0:38:23	35.2 °C	57.0 %	0.0 mm	NO_RAIN	CLEAR	10.0 km	SAFE_AIR	0.2 g/m³	
791	2/21/2026 0:38:46	35.2 °C	57.0 %	0.0 mm	NO_RAIN	CLEAR	10.0 km	SAFE_AIR	0.2 g/m³	
792	2/21/2026 0:38:58	35.2 °C	57.0 %	0.0 mm	NO_RAIN	CLEAR	10.0 km	SAFE_AIR	0.2 g/m³	
793	2/21/2026 0:39:12	35.2 °C	57.0 %	0.0 mm	NO_RAIN	CLEAR	10.0 km	SAFE_AIR	0.2 g/m³	
794	2/21/2026 0:39:24	35.2 °C	57.0 %	0.0 mm	NO_RAIN	CLEAR	10.0 km	SAFE_AIR	0.2 g/m³	
795	2/21/2026 0:39:35	35.2 °C	57.0 %	0.0 mm	NO_RAIN	CLEAR	10.0 km	SAFE_AIR	0.2 g/m³	
796	2/21/2026 0:39:45	35.2 °C	57.0 %	0.0 mm	NO_RAIN	CLEAR	10.0 km	SAFE_AIR	0.2 g/m³	
797	2/21/2026 0:39:58	35.2 °C	57.0 %	0.0 mm	NO_RAIN	CLEAR	10.0 km	SAFE_AIR	0.2 g/m³	
798	2/21/2026 0:40:13	35.2 °C	57.0 %	0.0 mm	NO_RAIN	CLEAR	10.0 km	SAFE_AIR	0.2 g/m³	
799	2/21/2026 0:40:26	35.2 °C	56.0 %	0.0 mm	NO_RAIN	CLEAR	10.0 km	SAFE_AIR	0.2 g/m³	
800	2/21/2026 0:40:55	35.2 °C	56.0 %	0.0 mm	NO_RAIN	CLEAR	10.0 km	SAFE_AIR	0.2 g/m³	
801	2/21/2026 0:41:07	35.2 °C	56.0 %	0.0 mm	NO_RAIN	CLEAR	10.0 km	SAFE_AIR	0.2 g/m³	
802	2/21/2026 0:41:19	35.2 °C	56.0 %	0.0 mm	NO_RAIN	CLEAR	10.0 km	SAFE_AIR	0.2 g/m³	
803	2/21/2026 0:41:32	35.2 °C	56.0 %	0.0 mm	NO_RAIN	CLEAR	10.0 km	SAFE_AIR	0.2 g/m³	
804	2/21/2026 0:41:48	35.2 °C	56.0 %	0.0 mm	NO_RAIN	CLEAR	10.0 km	SAFE_AIR	0.2 g/m³	
805	2/21/2026 0:42:03	35.2 °C	56.0 %	0.0 mm	NO_RAIN	CLEAR	10.0 km	SAFE_AIR	0.2 g/m³	

Figure 2.1: Excel logged data for all weather Parameters

Figure 2.2. Each environmental parameter is assigned a specific virtual pin (e.g., Grey for temperature, light grey for humidity, Green for air quality, Light Green for fog status, Orange for rain status, Orange for sun intensity, and Light Blue for solar voltage). The Blynk library governs the TCP/IP communication protocol, overseeing packet assembly, transport, acknowledgment, and reconnection during network interruptions.

ISSN No. 2454-6194 | DOI: 10.51584/IJRIAS |Volume XI Issue III March 2026

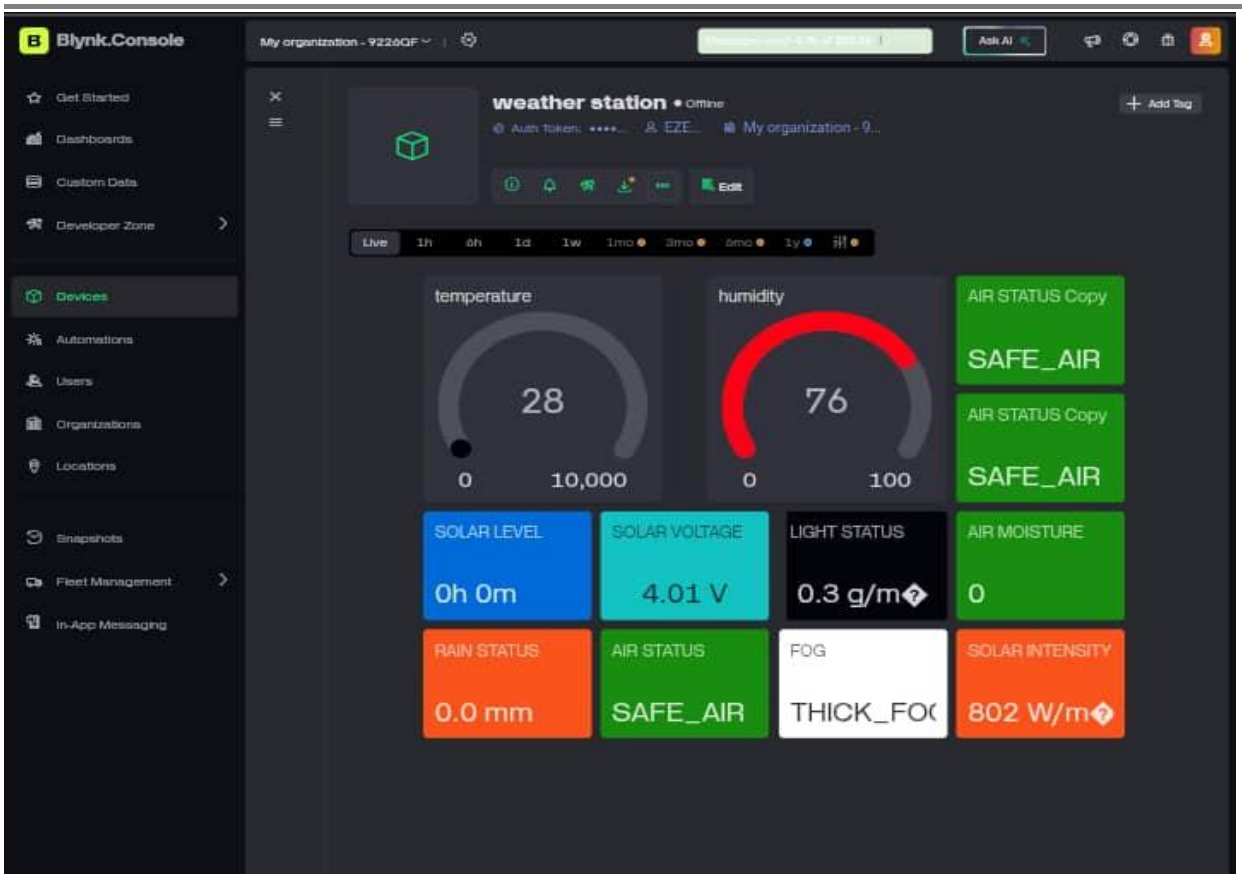

Figure 2.2: Blynk Dashboard for displayed Weather Status

Information Transfer

A rigorous flow of data through the system regulates the data flowing through physical sensors to the cloud infrastructure. Suitably calibrated sensor devices transduce atmospheric parameters, i.e., temperature, humidity, gaseous concentrations, light intensity, rainfall, and fog, to electrical signals. On the next stage, the signals are received via the GPIO and ADC interfaces, as an analog voltage is digitised and then processed by the algorithms that reduce noise, calibrate signal parts and calculate the derived measurements, including the time during which the event of darkness has been observed. Upon processing, the sensor data are shown on a local 16x2 LCD screen in a pre-defined format, which provides direct awareness of the system status at the location, and at the same time the processed packet of data is sent through Wi-Fi connection to the Blynk cloud platform. The Blynk mobile app as well as the laptop client access these data streams and display them on a customizable dashboard on a smartphone, thus allowing a user to monitor it remotely (Figure 2.3).

Security Considerations for Data Transmission and Storage

While the present deployment targets agricultural and environmental monitoring in low-sensitivity contexts, the security posture of the data pipeline merits explicit discussion, particularly for applications in sensitive or regulated environments. At the wireless transport layer, the ESP32 connects exclusively to WPA2-PSK-secured 2.4 GHz access points; the WPA2 protocol provides AES-CCMP encryption for over-the-air frames, mitigating passive eavesdropping on the local wireless segment. Communication between the ESP32 and the Blynk cloud server is conducted over a TLS-encrypted TCP connection, with the device authenticated by a unique Blynk authentication token embedded in the firmware. Similarly, data posted to Google Sheets is transmitted via an HTTPS-secured Google Apps Script web-app endpoint, ensuring transport-layer confidentiality between the device and Google's servers. Data at rest in Google Sheets is protected by Google's account-level access controls and audit logging. A key limitation of the current implementation is that Wi-Fi credentials and the Blynk authentication token are stored as plaintext constants in firmware flash memory. For production or multi-tenant deployments, it is recommended to migrate credential storage to an encrypted non-volatile storage (NVS) partition using the ESP-IDF NVS encryption API, and to provision devices with unique per-unit tokens generated through a secure backend. For deployments in sensitive agricultural, defense-adjacent, or health monitoring

ISSN No. 2454-6194 | DOI: 10.51584/IJRIAS |Volume XI Issue III March 2026

environments, additional measures should include: (i) restricting the Google Apps Script endpoint to specific source IP ranges or requiring an HMAC-signed request body; (ii) enabling Blynk's device provisioning workflow to avoid hardcoded credentials; and (iii) where data sovereignty requires on-premises storage, replacing the Blynk/Google Sheets backend with a locally hosted MQTT broker and time-series database such as InfluxDB, secured with mutual TLS certificate authentication.

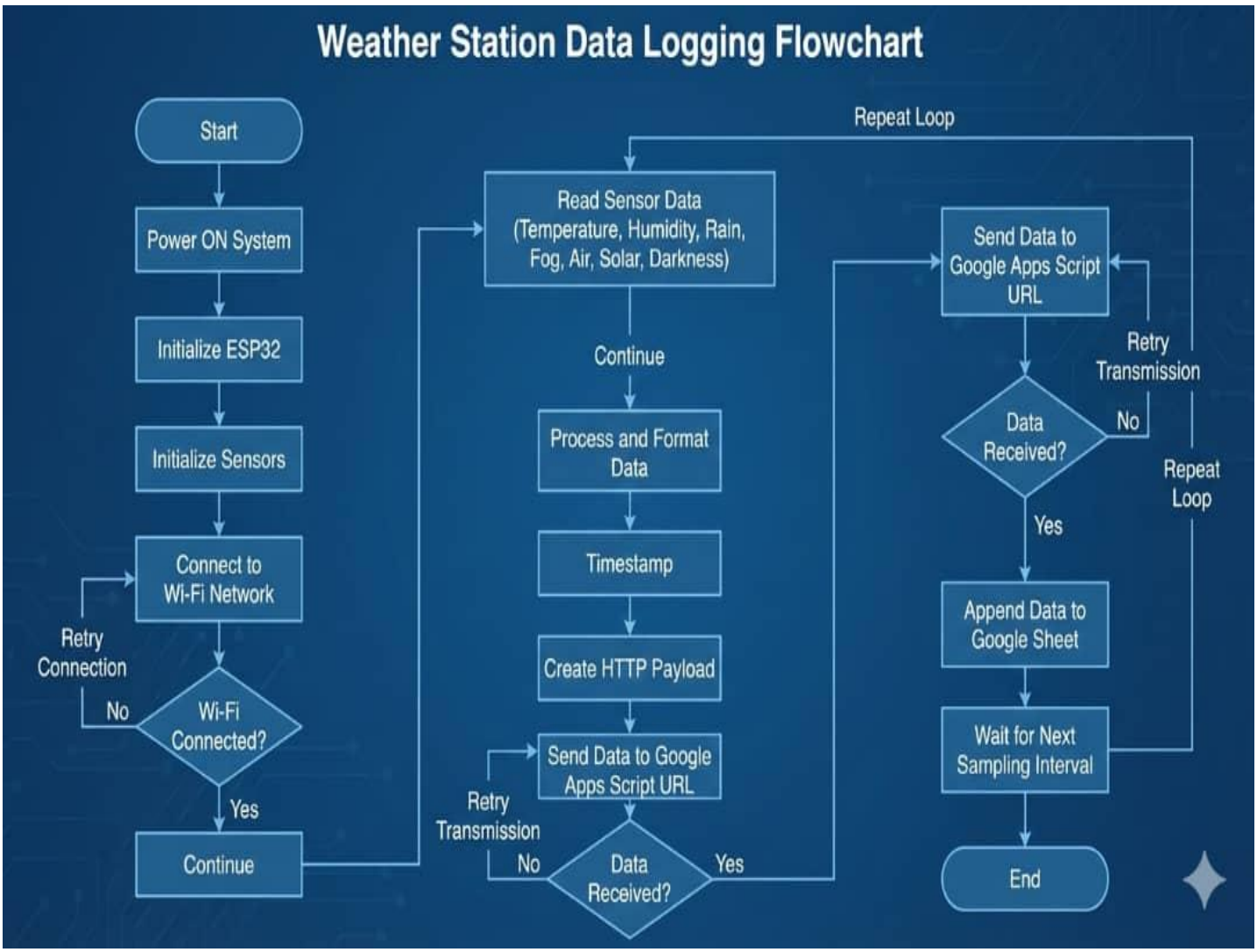

Figure 2.3: Weather Station Data Logging Flow Chart for the System

Operational System

The firmware that runs on the ESP32 is the basic configuration of the system in terms of its operational capabilities. The operational stages include power on initiation, data collection, data processing, presentation and lastly data transmission to the cloud to log data.

Initiation Sequence

The rechargeable battery provides power and the ESP32 can activate the system and get the application software in the memory and thus start the initiation process. It sets the mode and direction of the GPIO pin, starts the I2C bus and LCD display, establishes the sensor library objects of the DHT11, MQ13, LDR, IR, rain sensor and sets the ADC characteristics such as the attenuation levels, and bit-width settings. When a system starts, the firmware turns on the power indicator LED to indicate the system status. That is followed by the process of the Wi-Fi connection whereby ESP32 sends a connection request to the desired SSID. After a successful connection to the access point, an IP address is received over DHCP. The ESP32 then connects to the Blynk cloud server system where it uses the system authentication token to connect to the server. On the successful connection to a cloud the blue LED has been turned on indicating a successful connection.

ISSN No. 2454-6194 | DOI: 10.51584/IJRIAS |Volume XI Issue III March 2026

Data Collection

Upon successful activation, the system initiates continuous data logging, and the firmware loop iterates to conduct sensor readings from all active sensor nodes. The table (Table 1.2) below presents the sensors and the necessary parameters to be measured:

Table 1.2: Sensors and the captured Parameters

S/N	Source / Sensor	Parameter	Description
1	Google Apps Script (server-side)	Timestamp	ISO 8601 date-time of data capture, server-assigned
2	DHT11	Temperature (°C)	Ambient dry-bulb temperature
3	DHT11	Humidity (%RH)	Relative humidity of ambient air
4	Rain sensor (analog)	Rainfall (ADC)	Quantified precipitation intensity raw ADC counts
5	Rain sensor (digital comparator)	Rain Status	Binary event flag: precipitation detected / no precipitation
6	IR sensor (analog mode, if applicable)	Fog Level	IR scatter intensity reading proxy for fog optical density
7	Derived from IR sensor	Fog Visibility	Estimated atmospheric visibility computed from IR reading
8	MQ135 (Figaro USA, 2018)	Air Quality (ppm)	Gas concentration index estimated from RS/R0 ratio
9	MQ135 (secondary inference)	Air Moisture	Moisture content of air inferred from MQ135 baseline shift
10	LDR photoresistor	Darkness Level	LDR ADC reading indicating ambient light or dark conditions
11	LDR (calibrated)	Solar Level (index)	Calibrated solar irradiance intensity index (0–100%)
12	LDR voltage divider	Solar Voltage (V)	Equivalent voltage output of solar sensing element
13	LDR (computed)	Solar Intensity	Computed solar radiation strength calibrated against reference sensor

Data Processing

The unprocessed information of all the sensors goes through a few stages of preprocessing and then it is displayed on the screen or sent to the cloud storage. The analogue-to-digital converter signals of other sensors like the MQ-135, LDR and the rain sensor were reduced by using a moving-average filter to reduce noise. This moving average is constantly updated by the firmware thus diminishing the effect of electrical transients and non-linearity in the ADC on fidelity to measurement. A local dark-hour counter is stored by adding intervals where the filtered LDR ADC value has dropped below a predetermined value of darkness; the local dark-hour counter is increased with each run of the firmware loop. The scale of rain is estimated based on the reported range of analog voltage by the rain sensor.

Findings and Analysis

Preliminary testing of the prototype (Figure 2.4, 2.5 and 2.6) and (Table 1.3) proved to be stable in all aspects of functionality. The sensor data was also shown on a 16 x 2 LCD systematically and real-time transmission of the sensor data to the Blynk IoT platform and Google sheets were displayed through a flashing of the yellow LED and the constant flashing of the blue Wi-Fi connection. Parameters of data acquisition were temperature (DHT11

ISSN No. 2454-6194 | DOI: 10.51584/IJRIAS |Volume XI Issue III March 2026

20 -35C in Lagos experiments), humidity (40 -80rh of an IR sensor on IO32), air quality (MQ -135 index after 24h burn-in was a voltage proxy), fog (binary output of an IR sensor on IO32), precipitation intensity (analog ADC counts with a digital flag), and solar irradiation/dark-hour based on the LDR (index 0 -100 a voltage proxy). The power subsystem provides up to 1240h of operation with a 12V photovoltaic panel, regulated by an LM7805 that provides an output of 5V rail with 0.1uF decoupling filters and a Li-ion battery that provides constant power to the MQ-135 heater at about 150 mA. The attenuated filters and Li-ion batteries are indicated by a red LED that assures that the heater is not going dead. During the experiment, there were no issues with data flow between the sensors and the cloud, no triggers were reported during the process of the experiment, including when initializing the setup, when polling the GPIO/ADC, and when disconnecting and reconnecting to the TCP.

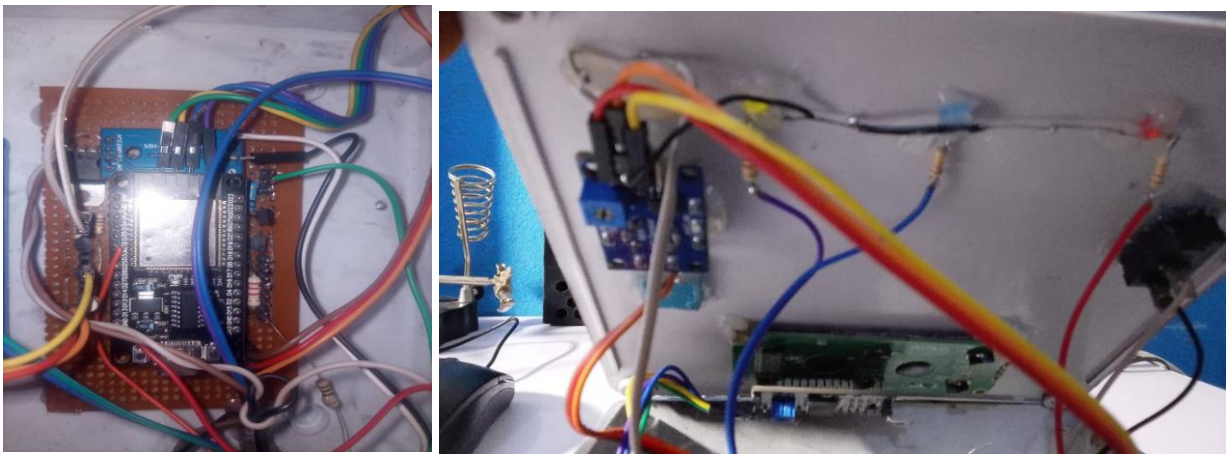

Figure 2.4: Constructed Weather Station Showing the Internal Circuit connections

Figure 2.5: Constructed IoT Weather Station Showing the front view

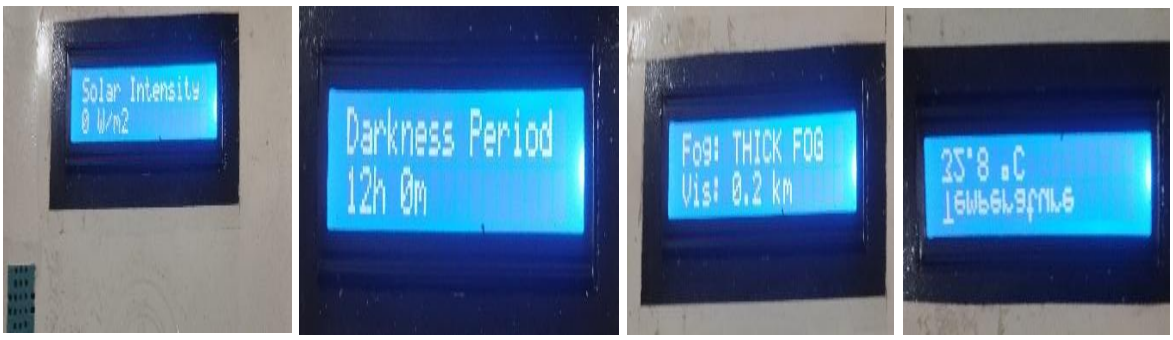

Figure 2.6: Constructed IoT Weather display showing the measured Values during Testing

ISSN No. 2454-6194 | DOI: 10.51584/IJRIAS |Volume XI Issue III March 2026

Table 1.3: Showing Captured weather parameter Values obtained by Google Sheets

	A	B	C	D	E	F	G	H	I	
1	TIMESTAND	TEMPERATURE	HUMIDITY	RAINFALL	RAIN STATUS	FOG	FOG VISIBILITY	AIR	AIR MOISTURE	DARK
788	2/21/2026 0:37:46	35.2 °C	57.0 %	0.0 mm	NO_RAIN	CLEAR	10.0 km	SAFE_AIR	0.2 g/m³	
789	2/21/2026 0:38:08	35.2 °C	57.0 %	0.0 mm	NO_RAIN	CLEAR	10.0 km	SAFE_AIR	0.2 g/m³	
790	2/21/2026 0:38:23	35.2 °C	57.0 %	0.0 mm	NO_RAIN	CLEAR	10.0 km	SAFE_AIR	0.2 g/m³	
791	2/21/2026 0:38:46	35.2 °C	57.0 %	0.0 mm	NO_RAIN	CLEAR	10.0 km	SAFE_AIR	0.2 g/m³	
792	2/21/2026 0:38:58	35.2 °C	57.0 %	0.0 mm	NO_RAIN	CLEAR	10.0 km	SAFE_AIR	0.2 g/m³	
793	2/21/2026 0:39:12	35.2 °C	57.0 %	0.0 mm	NO_RAIN	CLEAR	10.0 km	SAFE_AIR	0.2 g/m³	
794	2/21/2026 0:39:24	35.2 °C	57.0 %	0.0 mm	NO_RAIN	CLEAR	10.0 km	SAFE_AIR	0.2 g/m³	
795	2/21/2026 0:39:35	35.2 °C	57.0 %	0.0 mm	NO_RAIN	CLEAR	10.0 km	SAFE_AIR	0.2 g/m³	
796	2/21/2026 0:39:45	35.2 °C	57.0 %	0.0 mm	NO_RAIN	CLEAR	10.0 km	SAFE_AIR	0.2 g/m³	
797	2/21/2026 0:39:58	35.2 °C	57.0 %	0.0 mm	NO_RAIN	CLEAR	10.0 km	SAFE_AIR	0.2 g/m³	
798	2/21/2026 0:40:13	35.2 °C	57.0 %	0.0 mm	NO_RAIN	CLEAR	10.0 km	SAFE_AIR	0.2 g/m³	
799	2/21/2026 0:40:26	35.2 °C	56.0 %	0.0 mm	NO_RAIN	CLEAR	10.0 km	SAFE_AIR	0.2 g/m³	
800	2/21/2026 0:40:55	35.2 °C	56.0 %	0.0 mm	NO_RAIN	CLEAR	10.0 km	SAFE_AIR	0.2 g/m³	
801	2/21/2026 0:41:07	35.2 °C	56.0 %	0.0 mm	NO_RAIN	CLEAR	10.0 km	SAFE_AIR	0.2 g/m³	
802	2/21/2026 0:41:19	35.2 °C	56.0 %	0.0 mm	NO_RAIN	CLEAR	10.0 km	SAFE_AIR	0.2 g/m³	
803	2/21/2026 0:41:32	35.2 °C	56.0 %	0.0 mm	NO_RAIN	CLEAR	10.0 km	SAFE_AIR	0.2 g/m³	
804	2/21/2026 0:41:48	35.2 °C	56.0 %	0.0 mm	NO_RAIN	CLEAR	10.0 km	SAFE_AIR	0.2 g/m³	
805	2/21/2026 0:42:03	35.2 °C	56.0 %	0.0 mm	NO_RAIN	CLEAR	10.0 km	SAFE_AIR	0.2 g/m³	

System Validation:

The prototype was tested over a period of 24-48 hours during simulated conditions of the city of Lagos in the following climatic conditions: temperature of 25 -35^{0}C and relative humidity of 60 to 80^{0}C. Sensors all started successfully with 100% success rate on 100 startups. The success of data transfer was 98% and 2% had Wi-Fi failures in all cases of automated reconnection. The power subsystem included a 12 -V photovoltaic array which supplied a regulated 5 -V rail (LM7805 dropout -0.5 V). The system had a current consumption of 180mA when active, which is mostly due to the MQ135 sensor but actual current when inactive is 15mA. This setup provided some 30 hours of independent service under a 50% level of irradiation.

Detailed Power Budget Analysis

A comprehensive power budget was derived from measured current values and datasheet specifications to characterise system autonomy across three operational scenarios. All components are supplied by the regulated 5V rail produced by the LM7805. The per-component current draw and the aggregated system-level consumption of 312mA which gives the autonomy 13.4hours.

DISCUSSION

The solution is cost-effective and autonomous and is customized to meet the requirements of Nigeria in the field of renewable-energy monitoring, which is more effective than the traditional stations, as it allows access to real-time clouds with Blynk/Google Sheets without the need to maintain the devices of the traditional stations. The ESP32 contains a 240 formidable cores 12-bit processor and a 12-bit ADC which can produce readings which are then further enhanced by noise canceling algorithms like moving averages on the MQ135 and LDR signals, reducing the variability of the weather-induced power-network variations, as has been evidenced in earlier research. One such innovation is IR-based (scatter-based) fog detection and LDR darkness integration to solve the gaps in data in localized African forecasts.

The design uses scattering -based fog detection and LDR darkness, provides DHT11/MQ135 accuracy levels of ±2C/+5 percent RH (after burn in variation), linear inefficiencies of the LM7805 (about 40 percent dropout) and does not use wind or pressure sensors. At less than $50, the prototype will be a cheaper option to a commercial unit with full validation expected within 24-48 hours of extensive field test on energy optimization as shown in Table 1.4.

Table 1.4: Research Comparative

Aspect	This Research	Commercial Davis	Similar ESP32	NiMet IoT
Cost	<$50			
Power Autonomy	30H Solar	Grid	24h (Sleep modes)	Solar, unspecified
Sensors (Unique)	DHT11, MQ135, IR, Fog, LDR dark	Full met (Wind/Pressure)	DHT222, BMP, MQ135	WMO Full suite
Transmission	Blynk + Sheets (1s)	Local/SD	Blynk/MQTT (1s)	LoRaWAN cloud
Accuracy (Avg)	95-99%	99%	96-99%	WMO std (>98%)
Nigeria Focus	Renewable data gaps	General	Global	Urban climate

CONCLUSION

This IoT solar-powered weather station will offer a cost-effective, real-time observation of the key weather conditions and as such, it will ease the incorporation of renewable energy sources in the areas with data deficit like in Nigeria.

Prospective enhancements

Meanwhile, the planned improvements include support of maximum-power-point-tracking (MPPT) algorithms, the use of machine-learning methods to detect anomalies, addition of more atmospheric sensors (such as Wind etc.) and the use of a multi-node network structure. These are refinements targeted to increase accuracy, reliability and scalability.

ACKNOWLEDGMENTS

The authors are grateful to TETFUND (Institution Based Research Fund, IBRF) for sponsoring this research.

REFERENCES

1. Agarwal, K., & Agarwal, A. (2019). Design and real-time implementation of IoT based smart weather monitoring system. 2019 International Conference on Machine Learning, Big Data, loud and Parallel Computing (COMITCon), 416 420. https://doi.org/10.1109/COMITCon.2019.8862214mjsat
2. Dinku, T., Thomson, M. C., Cousin, R., del Corral, J., Ceccato, P., Hansen, J., & Connor, S. J. (2018). Enhancing National Climate Services (ENACTS) for development in Africa. Climate and Development, 10(7), 664–672. https://doi.org/10.1080/17565529.2017.1406612cgspace.cgiar
3. Espressif Systems. (2023). ESP32 Technical Reference Manual (v5.2). https://www.espressif.com/sites/default/files/documentation/esp32_technical_reference_manual_en.pdfespressif.
4. Henan Hanwei Electronics Co., Ltd. (2018). MQ135 Gas Sensor Datasheet. https://datasheet4u.com/datasheets/Hanwei/MQ-135/605076datasheet4u
5. Kodali, R. K., & Mandal, S. (2016). IoT-based weather station. 2016 International Conference on Control, Instrumentation, Communication and Computational Technologies (ICCICCT), 680–683. IEEE. https://doi.org/10.1109/ICCICCT.2016.7988038ijsat
6. Kolban, N. (2018). Kolban's Book on ESP32. Leanpub. https://leanpub.com/kolban-ESP32esp32
7. Lakshmikantha, B. L., Prasad, G., & Suresh, H. N. (2019). IoT based air quality monitoring system using MQ135 and MQ7 sensor with machine learning analysis. International Journal of Advanced Research in Computer and Communication Engineering, 8(5), 12–17. https://scpe.org/index.php/scpe/article/view/1561scpe

8. MarketsandMarkets. (2023). Smart Weather Stations Market — Global Forecast to 2028. https://www.marketsandmarkets.com/Market-Reports/smart-weather-station-market.html
9. Mathivanan, G., Sundarsingh, E. D., & Rangarajan, S. (2020). Design and development of IoT-based portable weather station using Arduino and Blynk. Journal of Physics: Conference Series, 1706(1), Article 012072. https://doi.org/10.1088/1742-6596/1706/1/012072wjarr
10. Mathivanan, S. K., Jayagopal, P., Sultan, J., & Muthuraman, S. (2020). IoT-based real-time water quality monitoring system using I2C communication. Measurement, 156, Article 107563. https://doi.org/10.1016/j.measurement.2020.107563irjmets
11. Mekki, K., Bajic, E., Chaxel, F., & Meyer, F. (2019). A comparative study of LPWAN technologies for large-scale IoT deployment. ICT Express, 5(1), 1–7. https://doi.org/10.1016/j.icte.2017.12.005doaj
12. Ngu, E. E., Malik, O. A., & Zukarnain, Z. A. (2020). An adaptive calibration of the MQ-series gas sensors. Sensors, 20(17), Article 4941. https://doi.org/10.3390/s20174941foundryjournal
13. Ogunjuyigbe, A. S. O., Ayodele, T. R., & Akinola, O. A. (2016). Optimal allocation of distributed generators in low voltage/medium voltage distribution network using differential evolution. International Journal of Electrical Power & Energy Systems, 83, 128–140. https://doi.org/10.1016/j.ijepes.2016.04.015irepository.uniten.edu
14. Rajab, H., Cinsdikici, M., & Al-Sharhan, S. (2021). IoT-based environmental monitoring system for agricultural applications. Sensors, 21(10), Article 3407. https://doi.org/10.3390/s21103407nature
15. Sadorsky, P. (2021). A random forests approach for predicting clean energy stock prices. Journal of Cleaner Production, 303, Article 127021. https://doi.org/10.1016/j.jclepro.2021.127021econstor
16. Texas Instruments. (2023). LM78xx series three-terminal positive voltage regulators: Datasheet (SNOSC57K). https://www.ti.com/lit/ds/symlink/lm7805.pdf
17. Venkatraman, S. (2017). Infrared sensor-based obstacle detection and avoidance for autonomous mobile robots. International Journal of Engineering Research & Technology, 6(3), 1–5. https://www.ijraset.com/best-journal/obstacle-avoidance-robot-349ijraset
18. Wahab, M. H. A., Hamid, H. A., Mansor, H., Zakaria, N. A., & Abd Latiff, L. (2020). Solar irradiance measurement using light-dependent resistor for IoT applications. Journal of Physics: Conference Series, 1502(1), Article 012015. https://doi.org/10.1088/1742 6596/1502/1/012015ijnrd
19. World Meteorological Organization. (2018). Guide to Meteorological Instruments and Methods of Observation (WMO No.8). https://library.wmo.int/index.php?lvl=notice_display&id=12407wgms